Journal of Magnetism and Magnetic Materials 537 (2021) 168179

Contents lists available at ScienceDirect

Journal of Magnetism and Magnetic Materials

journal homepage: www.elsevier.com/locate/jmmm

Lithiation of the Fe_2P-based magnetocaloric materials: A first-principles study

I. Batashev [a,*], G.A. de Wijs [b], N.H. van Dijk [a], E. Brück [a]

[a] Fundamental Aspects of Materials and Energy (FAME), Delft University of Technology, Delft 2629 JB, The Netherlands
[b] Radboud University, Institute for Molecules and Materials, Heyendaalseweg 135, Nijmegen 6525 AJ, The Netherlands

ARTICLE INFO

Keywords:
Magnetocaloric effect
DFT
First-principles calculations
Magnetic refrigeration
Curie temperature
Fe_2P

ABSTRACT

The physical properties of the extensively studied Fe_2P material family, well-known for its promising magnetocaloric qualities are greatly influenced by the unit-cell parameters of this hexagonal system. This sensitivity of the various magnetocaloric properties to structural parameters is particularly important for developing a material suitable for room-temperature magnetic refrigeration. A change in the unit cell, due to added elements can induce pronounced changes in the Curie temperature and the nature of the magnetic phase transition. Li belongs to a yet unexplored group of possible dopant elements – alkali metals, and exhibits an unusual behavior upon introduction to Fe_2P. We observe a preference to replace iron atoms, as opposed to the common tendency of non-magnetic dopants to replace phosphorus, leading to a strong influence on the magnetic structure. The addition of Li introduces a deformation of the unit cell with a small change in volume and a decrease in c/a ratio, while the same crystallographic phase is maintained over a relatively wide concentration range. We show that lithium has an exceptionally strong effect on the Curie temperature of Fe_2P reaching 800 K at 20% Li compared to 240 K for the undoped material.

1. Introduction

The concept of magnetic refrigeration is based on the magnetocaloric effect (MCE) defined as the reversible temperature change of the magnetic material upon adiabatic magnetization or demagnetization. This technique has great potential for being an environmentally friendly and energy-efficient replacement for the current vapor-cycle refrigeration technology [1,2]. Many theoretical and experimental studies on Fe_2P based compounds were reported over the past decades [3–5]. These materials remain, along with $La(Fe,Co,Si)_{13}$ and $La(Fe,Mn,Si)_{13}H$, among the most promising candidates for room temperature magnetic refrigeration. Among the definite advantages of the Fe_2P family are a small hysteresis, a large adiabatic temperature change and a high magnetic entropy change, as well as the possibility to tune the ferromagnetic (FM) to paramagnetic (PM) transition temperature by varying the composition of the material [6,7].

The ability to fine-tune T_C is especially important for practical applications, both for cooling and energy conversion purposes. The magnetic and magnetocaloric properties of these materials are heavily influenced by the lattice parameters [8]. This stems from the mixed magnetism [9] observed in Fe_2P-based materials, where the magnetic structure has two different magnetic sublattices with large and moderate moments. The recent experimental measurement suggests values of $2.05\mu_B$ and $0.8\mu_B$ at 10 K [10]. The exchange interaction varies greatly for different Fe–Fe pairs, depending on the distances between the respective atoms. This, in combination with the fact that the strongly magnetic sublattice enhances the weaker magnetic sublattice, leads to a large sensitivity of the magnetism to structural changes. Previously, several approaches were tested to control T_C in this material system, while maintaining the optimal magnetocaloric properties, through substitutions and additions of elements such as Si, As, B [11–13]. These theoretical and experimental studies revealed that a decrease in the c/a ratio causes an upward shift of T_C.

In this work, the effect of lithiation of Fe_2P on the magnetization, critical temperature and structural parameters has been investigated within the framework of the density functional theory. Pure Fe_2P was selected instead of $(Mn,Fe)_2(P, Si)$ to minimize the number of possible factors of interest during the modelling. Since the materials within this family tend to share common features the trend observed for Fe_2P is expected to be transferable to its more complex relatives.

* Corresponding author.
E-mail address: i.batashev@tudelft.nl (I. Batashev).

https://doi.org/10.1016/j.jmmm.2021.168179
Received 10 November 2020; Received in revised form 11 March 2021; Accepted 2 June 2021
Available online 9 June 2021

2. Computational details

First-principles electronic structure calculations in the framework of the density functional theory (DFT) were performed. The Vienna *ab initio* simulation package (VASP) [14,15] in the projector augmented-wave (PAW) method [16,17] was employed to perform the DFT calculations using the generalized gradient approximation of Perdew-Burke-Ernzerhof (PBE) [18] for the exchange-correlation functional. In all calculations the Fe $1s, 2s, 2p, 3s$ and $3p$ were treated as core electrons. And for P the $1s, 2s$, and $2p$ were treated as core electrons. Lastly, for Li, the $1s$ electrons were kept frozen. The structural degrees of freedom were fully relaxed on a Γ-centred k-grid of $7 \times 7 \times 11$. The k-space integrations were performed with the Methfessel-Paxton method [19] of second order with a smearing width of 0.05 eV. The lattice parameters and atomic positions were relaxed for a force convergence tolerance of 0.1 meV/Å, while for total energies the tolerance was 1 μeV. The kinetic energy cutoff was set at 600 eV for $(Fe,Li)_2P$ and 450 eV for Fe_2P.

The starting material Fe_2P has $P\bar{6}2m$ symmetry (space group 189) and a hexagonal structure with two crystallographic sites ($3g$, $3f$) occupied by Fe atoms and two sites ($2c, 1b$) occupied by P atoms, see Fig. 1. The undoped unit cell of Fe_2P consists of three formula units with lattice parameters $a = 5.811$ Å and $c = 3.419$ Å, as obtained after optimization (in agreement with the experimental values $a = 5.867$ Å, $c = 3.458$ Å reported in Ref. [20]). The Fe atoms on the two crystallographic sites are magnetic with $3g$ being strongly magnetic and $3f$ moderately magnetic. As a result, Fe_2P exhibits mixed magnetism as mentioned before.

In order to study the effect of Li doping on Fe_2P, a $2 \times 2 \times 2$ supercell was utilized. Lithiation was modelled in the following way: a set of computations was performed with a single Li atom placed on various possible atomic sites in the supercell, comparing the resulting energies to determine the optimal position for the first Li. The same process is then repeated for each subsequent Li atom, covering a doping range from 0% to 25% in steps of ∼ 2%.

In order to model the PM state, a smaller $2 \times 2 \times 1$ supercell was doubled along the z direction, again making a $2 \times 2 \times 2$ supercell, but this time an antiparallel magnetic ordering was imposed: Moments inside each $2 \times 2 \times 1$ layer were aligned in the same direction, whereas the moments in adjacent $2 \times 2 \times 1$ layers were opposite. Thus one has alternating spin-up and spin-down blocks along the c direction forming an AFM structure with a total magnetic moment of zero (see Supplemental material). Such approximation is deemed reasonable for Fe_2P in [21]. This specific AFM supercell was chosen as the one with the lowest energy after a set of energy calculations for various AFM configurations. Experimental data for this system shows that the Fe moment decreases as temperature increases further above T_C [22,23]. This indicates the presence of short-range order closely above the transition temperature, which vanishes at higher temperatures, leading to a purely paramagnetic state. Therefore we consider AFM structures with low magnetic moments as most reasonable approximation of the PM state. Tested structures include $2 \times 2 \times 2$ supercell with antiparallel alignment between unit cells in a-direction, in checkerboard pattern (both within ab-plane and across c-direction) and possible periodicities of the antiparallel alignment along c-direction in a $1 \times 2 \times 4$ supercell.

The size of supercell determines the number of Fe atoms available for substitutions and consequently the precision of doping steps. The choice of $2 \times 2 \times 2$ supercell with the antiparallel layers (c-direction) therefore leads to a bigger step in Li doping (4%), as spin-up and spin-down layers must have the same atomic composition, only with an opposite direction for the magnetic moments.

3. Results and discussion

To investigate site preference for lithiated Fe_2P one Li atom was placed on either of the four possible crystallographic sites of the Fe_2P unit cell or on interstitial positions. The interstitial positions were included to account for the scenario reported for boron atoms in the case of MnFe(P,As,B) [24,25]. Energies are presented for three such interstitial positions: $6k, 6j$ and $2d$. Calculations with the inclusion of Li on other possible positions failed to converge to a stable structure. The energy cost E_f of forming the lithiated compound is calculated as the difference between the energies of the lithiated ($E_{\text{lithiated}}$) and pure (E_{pure}) compounds minus the chemical potential of the Li atom (μ_{Li}) plus the chemical potential of the atom s that Li substitutes for (μ_s), if applicable. So it is

$$E_f = E_{\text{lithiated}} + \mu_s - \left(E_{\text{pure}} + \mu_{\text{Li}}\right) \quad (1)$$

in case of a substitution and

$$E_f = E_{\text{lithiated}} - E_{\text{pure}} - \mu_{\text{Li}} \quad (2)$$

if Li goes to an interstitial site. Chemical potentials are obtained by first optimizing BCC iron, BCC lithium and tetrahedral phosphorus and then taking the total energy per atom.

According to the results obtained after full structural relaxation (Table 1) lithium prefers to occupy the $3g$ positions replacing iron, contrary to the usual preference for non-magnetic atoms to replace phosphorus or reside on interstitial positions. A preference for the $3g$ positions is maintained for the whole range of Li doping. This is likely due to the large size of the Li atom, as the $3g$ site has the biggest distances to neighbouring atoms, allowing for the inclusion of lithium with the smallest deformation of the unit cell. As can be seen from Fig. 2, during lithiation subsequent replacements occur for atoms that already have Li as their neighbour in the same plane (results for every step of lithiation can be found in the Supplemental material).

The evident non-random nature of the substitutions has several consequences: firstly, the tendency to prefer positions on the same $3g$ plane affects the magnetic interactions of the compound during lithiation, as will be described in detail in the following. Secondly, the formation of Li clusters leads to destabilization of the Fe_2P structure, thereby limiting the maximum amount of lithium that could be introduced in the system. According to the calculations, it is favourable for Li to enter Fe_2P, replacing up to 25% of the iron atoms (for higher concentrations E_f becomes positive). This, however, is only valid if no

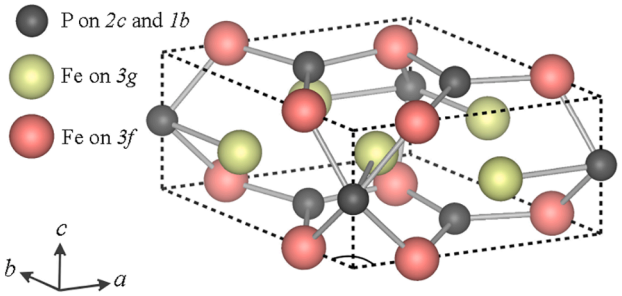

Fig. 1. Schematic representation of Fe_2P.

Table 1
Energy cost of forming lithiated compound for different site choices of Li substitution.

Position	E_f (eV)
$3g$ (Fe2)	−2.65
$3f$ (Fe1)	−1.96
$6k$ (I)	−0.71
$2d$ (I)	−0.71
$6j$ (I)	−0.61
$2c$ (P1)	0.8
$1b$ (P2)	0.8

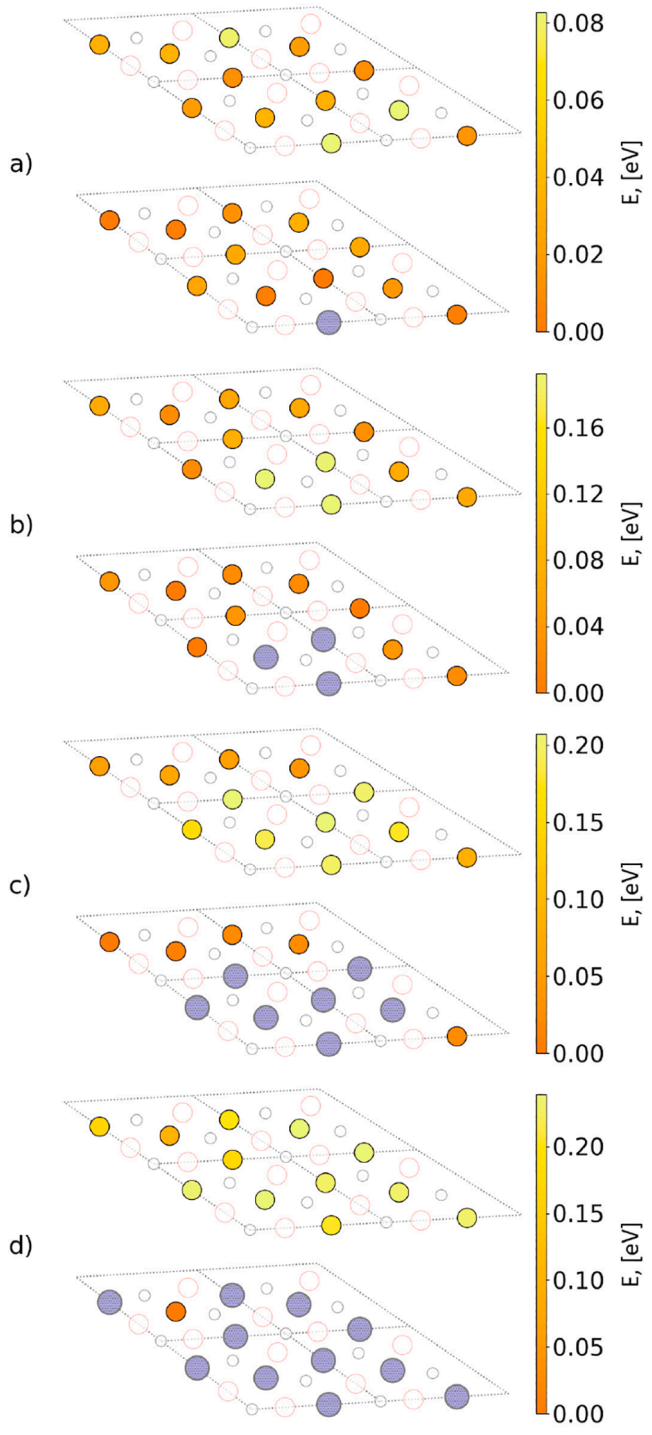

Fig. 2. Progress of lithiation for the 3*g* position in $Fe_{2-x}Li_xP$ shown for substitutions of 2(a), 4(b), 8(c) and 12(d) Fe atoms by Li. The colourmap indicates the energy of the substitution for this doping step. Energies are relative to the energy of the most preferred position (dark orange) at each step. Li atoms are marked with lilac circles. The structural deformation is not depicted for simplicity.

secondary phases are taken into account. $Fe_{2-x}Li_xP$ is likely to decompose into tetragonal Fe_3P and LiP at even lower Li content with some other possibilities as described in Ref. [26].

The process of lithiation is accompanied by an overall decrease in the magnetization as the iron atoms on the 3*g* positions, which carry the biggest moment of about $2.23\mu_B$, are replaced by non-magnetic Li atoms. The remaining Fe atoms on the 3*g* positions have their average moment progressively lowered to $1.99\mu_B$. The average moment on the 3*f* position is gradually decreasing from $0.83\mu_B$ to $0.66\mu_B$, as the 3*g* sublattice is disrupted. This can be explained by the fact that lithiation creates a non-magnetic buffer between the magnetic sublattices and effectively weakens the corresponding exchange interactions responsible for the mixed magnetism.

Preliminary experimental results indicate that small amounts of Li cause a sharp increase in the Curie temperature both for Fe_2P and for $(Fe, Mn)_2(P, Si)$ [27]. Details on experimental results can be found in the Supplemental material (Table S1). In order to verify this observation and estimate the transition temperature at different stages of lithiation the approach described in [28,29] was used. The mean-field approximation allows evaluation of the critical temperature by the (positive) total energy difference ΔE between the disordered state and the ordered ferromagnetic state. This energy difference is obtained by calculating total energies for the system in the AFM (E_{AFM}) and the FM (E_{FM}) state. Thus we calculate T_C as

$$T_C = \frac{2}{3(1-n)}\frac{\Delta E}{k_B} = \frac{2}{3(1-n)}\frac{(-E_{FM}+E_{AFM})}{k_B} \quad (3)$$

where n is the concentration of the non-magnetic elements. This simplified approach was used as a fast method to qualitatively estimate the effect of lithiation on T_C. Furthermore, due to the presence of two magnetic sites and the gradual introduction of Li, which disrupts crystal and magnetic symmetry of the system, the commonly used method to calculate T_C by mapping energies onto an effective Hamiltonian becomes rather cumbersome to utilize. Even with this approximation, the resulting Curie temperature for Fe_2P of 236K lies quite close to the experimental value of 217 K [30]. This indicates a reasonably good balance between computational effort and the obtained result for this method. While this mean field formulation shows reasonable agreement for certain systems [31,29], it is known to lead to significant errors in the calculated T_C for systems with short-range exchange interactions strongly diluted with non-magnetic elements [32]. In the case of $Fe_{2-x}Li_xP$, technically 25% (half of the 3*g* positions occupied in $2 \times 2 \times 1$ supercell) substitution is still above the percolation threshold, but the preference of Li for clustering discussed above, together with the fact that the 3*g* sublattice plays a major role in forming magnetic ordering in this system makes the T_C obtained for high percentages of Li less reliable and likely to be overestimated. The calculated values of T_C for different amounts of Li are presented in Fig. 3. The introduction of Li causes a sharp linear increase in T_C, which continues until a maximum T_C of

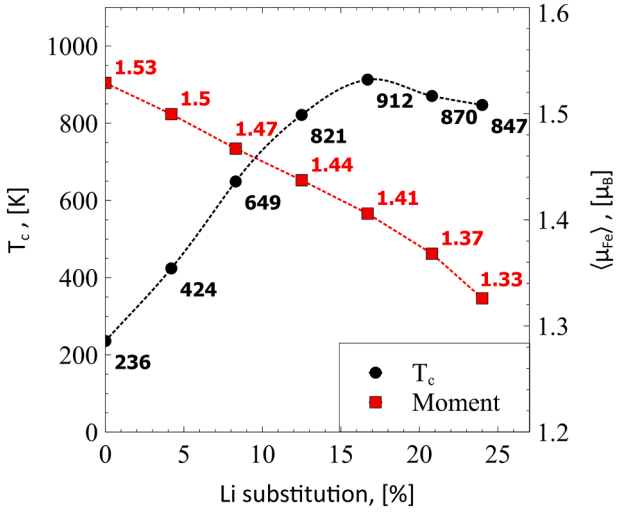

Fig. 3. Dependence of the critical temperature T_C and average magnetic moment of Fe on both sites as a function of the lithium content. Lines are a guide to the eye.

about 900 K is reached when 16.7% of the iron atoms are replaced by Li. For higher Li substitutions T_C slowly decreases. Thus, Li substitutions show the largest increase in T_C among all substitutions reported for this compound [13] with a rate of approximately 45 K/at.%

The change in lattice parameters as a result of the lithiation is presented in Table 2. An increase in lattice parameter a and a decrease in c leads to a decrease in the c/a ratio, while the volume of the unit cell exhibits a slight increase (Fig. 4). The changes in the unit cell volume are rather small since the deformations in the *ab* plane and along the *c* axis partially compensate for each other. As presented earlier, in the later stages of the lithiation the Li atoms occupy most of the positions in one of the 3*g* sublayers in the supercell, and therefore the last few substitutions no longer cause further deformations. As a result, the calculated values for the a parameter remain practically constant in these later stages.

Both an increase in volume and a reduction in the c/a ratio were previously reported as factors that lead to a higher critical temperature in Fe_2P-based materials [13], and $Fe_{2-x}Li_xP$ appears to follow this trend. This effect is further studied in [33], where heavy dependence of the metamagnetic transition of 3*f* species on the local environment is demonstrated. The variation in the Curie temperature is primarily controlled by the change in c/a ratio, and the main source of this variation in the case of $Fe_{2-x}Li_xP$ can be linked to the distance between magnetic sublattices. The exchange parameters in this system greatly decrease with the distance as shown in [34]. Among them the parameters for interlayer 3*g*-3*f* and 3*g*-3*g* interactions are most affected by structural changes. As Li replaces Fe on the 3*g* position, the decrease in *c* parameter leads to the enhancement of the interlayer interactions which, in turn causes to an increase in T_C. As seen from Figs. 3 and 5 for a moderate lithiation the changes in critical temperature can be correlated directly to the variation in c/a ratio.

4. Conclusions

In this paper, we have investigated the effect of lithium doping on the magnetic and structural properties of Fe_2P by first-principles calculations. Two magnetic sublattices, one with a large moment ($2.33\mu_B$ on the 3*g* positions) and the other with a moderate moment ($0.83\mu_B$ on 3*f* positions) are present in Fe_2P system. It is found that Li partially substitutes Fe on the 3*g* site. For $Fe_{2-x}Li_xP$ we present the development of the Curie temperature and the magnetic moments on the Fe sites as a function of the Li content. Since Li prefers the 3*g* positions a relatively large magnetic moment is lost on each substitution, causing an overall reduction in the magnetization. The formation of Li clusters at higher doping content further disrupts magnetic structure. At the same time even a small amount of lithium doping leads to a drastic increase in T_C. This is primarily the result of structural changes, in the c/a ratio in particular, as the *c* parameter decreases with increasing Li content, whereas the a parameter increases.

This study offers a novel route to optimize critical temperature and confirms the extreme sensitivity of the magnetic properties of the Fe_2P based material family to structural changes, demonstrating the importance of a proper understanding of the doping mechanism for the development of these magnetocaloric materials.

Data availability

The data supporting this study's findings are available in the article.

CRediT authorship contribution statement

I. Batashev: Investigation, Formal analysis, Validation, Writing - original draft. **G.A. de Wijs:** Resources, Methodology, Writing - review & editing. **N.H. van Dijk:** Supervision, Writing - review & editing. **E. Brück:** Conceptualization, Funding acquisition, Project administration.

Table 2
Structural parameters and average magnetic moments of Fe on the 3*g* and 3*f* sites during the lithiation of Fe_2P.

Li (at.%)	a (Å)	c (Å)	V (Å^3)	c/a	$\langle\mu_{3g}\rangle$ (μ_B)	$\langle\mu_{3f}\rangle$ (μ_B)
0	5.81	3.42	99.98	0.588	2.23	0.83
4.2	5.83	3.42	100.23	0.586	2.17	0.83
8.3	5.85	3.41	100.46	0.583	2.13	0.81
12.5	5.85	3.40	100.71	0.580	2.10	0.78
16.7	5.88	3.39	100.99	0.577	2.06	0.75
20.8	5.88	3.38	101.35	0.575	2.02	0.71
24	5.88	3.36	101.53	0.571	1.99	0.66

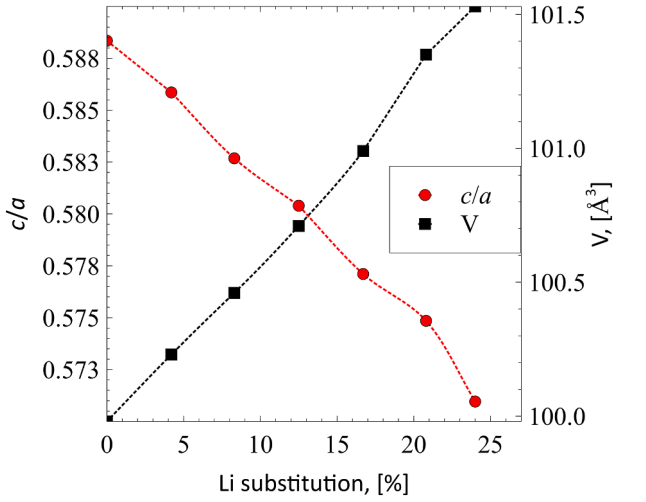

Fig. 4. Dependence of the c/a ratio and the volume V on the lithium content. Lines are a guide to the eye.

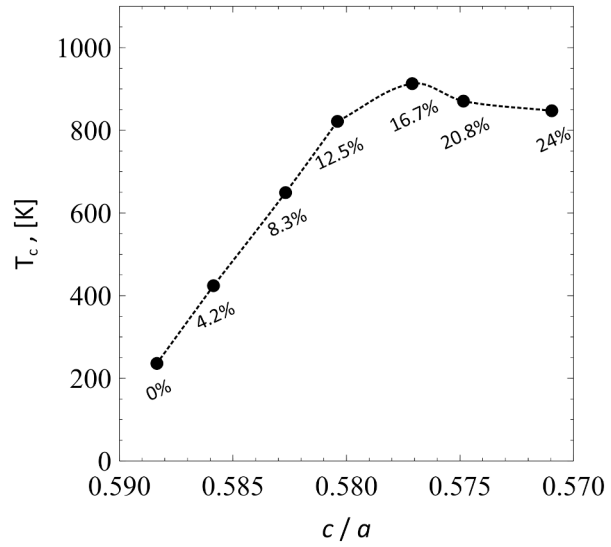

Fig. 5. Dependence of the critical temperature on the c/a ratio. The lithium content is labelled for each point. Lines are a guide to the eye.

Declaration of Competing Interest

The authors declare that they have no known competing financial interests or personal relationships that could have appeared to influence the work reported in this paper.

Acknowledgement

The authors thank Mischa van Diepen and Kelvin Lindeborg for their assistance. This work is part of the research project number 16VAL56, which is financed by the Dutch Research Council (NWO).

Appendix A. Supplementary data

Supplementary data associated with this article can be found, in the online version, at https://doi.org/10.1016/j.jmmm.2021.168179.

References

[1] E. Brück, Developments in magnetocaloric refrigeration, J. Phys. D Appl. Phys. 38 (23) (2005) R381–R391, https://doi.org/10.1088/0022-3727/38/23/R01.
[2] K. Gschneidner, V. Pecharsky, Thirty years of near room temperature magnetic cooling: where we are today and future prospects, Int. J. Refrig. 31 (6) (2008) 945–961, https://doi.org/10.1016/j.ijrefrig.2008.01.004.
[3] D.T. Cam Thanh, E. Brück, N.T. Trung, J.C.P. Klaasse, K.H.J. Buschow, Z.Q. Ou, O. Tegus, L. Caron, Structure, magnetism, and magnetocaloric properties of $MnFeP_{1-x}Si_x$ compounds, J. Appl. Phys. 103 (7) (2008) 07B318, https://doi.org/10.1063/1.2836958.
[4] E. Brück, M. Ilyn, A. Tishin, O. Tegus, Magnetocaloric effects in $MnFeP_{1-x}As_x$-based compounds, J. Magn. Magn. Mater. 290–291 (2005) 8–13, https://doi.org/10.1016/j.jmmm.2004.11.152.
[5] H. Yamada, K. Terao, First-order transition of Fe_2P and anti-metamagnetic transition, Phase Trans. 75 (1–2) (2002) 231–242, https://doi.org/10.1080/01411590290023120.
[6] N.H. Dung, L. Zhang, Z.Q. Ou, E. Brück, Magnetoelastic coupling and magnetocaloric effect in hexagonal Mn-Fe-P-Si compounds, Scr. Mater. 67 (12) (2012) 975–978, https://doi.org/10.1016/j.scriptamat.2012.08.036.
[7] X.F. Miao, L. Caron, P. Roy, N.H. Dung, L. Zhang, W.A. Kockelmann, R.A. de Groot, N.H. van Dijk, E. Brück, Tuning the phase transition in transition-metal-based magnetocaloric compounds, Phys. Rev. B 89 (17) (2014), 174429, https://doi.org/10.1103/PhysRevB.89.174429.
[8] Z. Ou, L. Caron, N. Dung, L. Zhang, E. Brück, Interstitial boron in MnFe(P, As) giant-magnetocaloric alloy, Results Phys. 2 (2012) 110–113, https://doi.org/10.1016/j.rinp.2012.09.005.
[9] N.H. Dung, Z.Q. Ou, L. Caron, L. Zhang, D.T.C. Thanh, G.A. de Wijs, R.A. de Groot, K.H.J. Buschow, E. Brück, Mixed magnetism for refrigeration and energy conversion, Adv. Energy Mater. 1 (6) (2011) 1215–1219, https://doi.org/10.1002/aenm.201100252.
[10] J. Cedervall, M.S. Andersson, E.K. Delczeg-Czirjak, D. Iuan, M. Pereiro, P. Roy, T. Ericsson, L. Häggström, W. Lohstroh, H. Mutka, M. Sahlberg, P. Nordblad, P. P. Deen, Magnetocaloric effect in Fe_2P: magnetic and phonon degrees of freedom, Phys. Rev. B 99 (2019), 174437, https://doi.org/10.1103/PhysRevB.99.174437.
[11] E.K. Delczeg-Czirjak, L. Delczeg, M.P.J. Punkkinen, B. Johansson, O. Eriksson, L. Vitos, Ab initio study of structural and magnetic properties of Si-doped Fe_2P, Phys. Rev. B 82 (8) (2010), 085103, https://doi.org/10.1103/PhysRevB.82.085103.
[12] Y.H. Z. Dechang, T. Zhucai, Z. Zhigang, Z. Xichun, L. Zhongwu, Patent CN102881393A (2013).
[13] E.K. Delczeg-Czirjak, Z. Gercsi, L. Bergqvist, O. Eriksson, L. Szunyogh, P. Nordblad, B. Johansson, L. Vitos, Magnetic exchange interactions in B-, Si-, and As-doped Fe_2P from first-principles theory, Phys. Rev. B 85 (22) (2012), 224435, https://doi.org/10.1103/PhysRevB.85.224435.
[14] G. Kresse, J. Hafner, Ab initio molecular dynamics for liquid metals, Phys. Rev. B 47 (1) (1993) 558–561, https://doi.org/10.1103/PhysRevB.47.558.
[15] G. Kresse, J. Furthmüller, Efficiency of ab-initio total energy calculations for metals and semiconductors using a plane-wave basis set, Comput. Mater. Sci. 6 (1) (1996) 15–50, https://doi.org/10.1016/0927-0256(96)00008-0.
[16] P.E. Blöchl, Projector augmented-wave method, Phys. Rev. B 50 (24) (1994) 17953–17979, https://doi.org/10.1103/PhysRevB.50.17953.
[17] G. Kresse, D. Joubert, From ultrasoft pseudopotentials to the projector augmented-wave method, Phys. Rev. B 59 (3) (1999) 1758–1775, https://doi.org/10.1103/PhysRevB.59.1758.
[18] J.P. Perdew, K. Burke, M. Ernzerhof, Generalized gradient approximation made simple, Phys. Rev. Lett. 77 (18) (1996) 3865–3868, https://doi.org/10.1103/PhysRevLett.77.3865.
[19] M. Methfessel, A.T. Paxton, High-precision sampling for Brillouin-zone integration in metals, Phys. Rev. B 40 (6) (1989) 3616–3621, https://doi.org/10.1103/PhysRevB.40.3616.
[20] B. Carlsson, M. Gölin, S. Rundqvist, Determination of the homogeneity range and refinement of the crystal structure of Fe_2P, J. Solid State Chem. 8 (1) (1973) 57–67, https://doi.org/10.1016/0022-4596(73)90021-2.
[21] P. Roy, E. Torun, R.A. de Groot, Effect of doping and elastic properties in $(Mn, Fe)_2(Si, P)$, Phys. Rev. B 93 (9) (2016) 94110, https://doi.org/10.1103/PhysRevB.93.094110.
[22] N.H. Dung, L. Zhang, Z.Q. Ou, L. Zhao, L. van Eijck, A.M. Mulders, M. Avdeev, E. Suard, N.H. van Dijk, E. Brück, High/low-moment phase transition in hexagonal Mn-Fe-P-Si compounds, Phys. Rev. B 86 (4) (2012), 045134, https://doi.org/10.1103/PhysRevB.86.045134.
[23] H. Yibole, F. Guillou, L. Caron, E. Jiménez, F.M.F. de Groot, P. Roy, R. de Groot, N. H. van Dijk, E. Brück, Moment evolution across the ferromagnetic phase transition of giant magnetocaloric $(Mn, Fe)_2(P, Si, B)$, Phys. Rev. B 91 (1) (2015), 014429, https://doi.org/10.1103/PhysRevB.91.014429.
[24] F. Guillou, H. Yibole, G. Porcari, E. Brück, Boron addition in MnFe(P, Si) magnetocaloric materials: interstitial vs. substitutional scenarii, Phys. Status Solidi 11 (5–6) (2014) 1007–1010, https://doi.org/10.1002/pssc.201300569.
[25] F. Guillou, G. Porcari, H. Yibole, N. van Dijk, E. Brück, Taming the first-order transition in giant magnetocaloric materials, Adv. Mater. 26 (17) (2014) 2671–2675, https://doi.org/10.1002/adma.201304788.
[26] S.P. Ong, L. Wang, B. Kang, G. Ceder, Li-Fe-P-O 2 phase diagram from first principles calculations, Chem. Mater. 20 (5) (2008) 1798–1807, https://doi.org/10.1021/cm702327g.
[27] K.G. Lindeborg, First Lithiation of the Fe2P-based Magnetocaloric Materials., Master's thesis, TU Delft, the Netherlands, 2018.
[28] F. Körmann, D. Ma, D.D. Belyea, M.S. Lucas, C.W. Miller, B. Grabowski, M.H. F. Sluiter, Treasure maps for magnetic high-entropy-alloys from theory and experiment, Appl. Phys. Lett. 107 (14) (2015), 142404, https://doi.org/10.1063/1.4932571.
[29] K. Sato, L. Bergqvist, J. Kudrnovský, P.H. Dederichs, O. Eriksson, I. Turek, B. Sanyal, G. Bouzerar, H. Katayama-Yoshida, V.A. Dinh, T. Fukushima, H. Kizaki, R. Zeller, First-principles theory of dilute magnetic semiconductors, Rev. Mod. Phys. 82 (2) (2010) 1633–1690, https://doi.org/10.1103/RevModPhys.82.1633.
[30] L. Lundgren, G. Tarmohamed, O. Beckman, B. Carlsson, S. Rundqvist, First order magnetic phase transition in Fe_2P, Phys. Scr. 17 (1) (1978) 39–48, https://doi.org/10.1088/0031-8949/17/1/008.
[31] M. Ležaić, P. Mavropoulos, S. Blügel, First-principles prediction of high Curie temperature for ferromagnetic bcc-Co and bcc-FeCo alloys and its relevance to tunneling magnetoresistance, Appl. Phys. Lett. 90 (8) (2007), 082504, https://doi.org/10.1063/1.2710181.
[32] K. Sato, W. Schweika, P.H. Dederichs, H. Katayama-Yoshida, Low-temperature ferromagnetism in (Ga, Mn)N: ab initio calculations, Phys. Rev. B 70 (20) (2004), 201202, https://doi.org/10.1103/PhysRevB.70.201202.
[33] Z. Gercsi, E.K. Delczeg-Czirjak, L. Vitos, A.S. Wills, A. Daoud-Aladine, K. G. Sandeman, Magnetoelastic effects in doped Fe_2P, Phys. Rev. B 88 (2) (2013), 024417, https://doi.org/10.1103/PhysRevB.88.024417.
[34] X. Liu, J. Ping Liu, Q. Zhang, Z. Altounian, Fe magnetic moment formation and exchange interaction in Fe_2P: a first-principles study, Phys. Lett. A 377 (9) (2013) 731–735, https://doi.org/10.1016/j.physleta.2013.01.019.